Knudsen's Cosine Law and Random Billiards

R. Feres* and G. Yablonsky†

Abstract

This article lays the groundwork for understanding the details of gas transport in the so-called Knudsen regime, particularly during the early, non-stationary stages of the transport process. A simple mathematical model of gas-surface interaction is introduced, which is both fairly general and sufficiently explicit to permit a detailed analysis. The model, which we call a *random billiard*, is an example of a random dynamical system based on the idea of a billiard system with geometric microstructure. Among the main results, we show that Knudsen's cosine law is a stationary probability distribution of post-collision velocities, although not always the unique one. Through numerical experiments with a variety of microgeometries we also provide some insight concerning the approach to stationarity.

1 Introduction and Overview

Studies about gas flow in the Knudsen regime are of interest to researchers in many areas of physics, chemistry and technology, from traditional heterogeneous catalytic processes over porous catalysts, to molecular transport processes in nano-structured materials, to rarefied gas processes in atmosphere and space ([KR, Ke]). We note, in particular, [SNQ], which is concerned with diffusion in carbon nanotubes. The statistical basis of the subject, however, particularly regarding non-equilibrium properties, have not been much studied and are poorly developed. In this paper we take a closer look at some basic questions, particularly regarding the so-called *Knudsen cosine law*, which we recall next.

Knudsen's experimental study of flows of rarefied gases through tubes, which he initiated around 1907, was among the first designed to test the consequences of the kinetic theory of gases. (See [Kn].) Rarefaction is conveniently defined by saying that the Knudsen number, λ/r, is large, where λ is the mean free path and r is a characteristic length such as the diameter of the tube. For large Knudsen numbers relatively few gas molecules collide with each other compared to the number of collisions between molecules and the wall of the tube.

*Dept. of Mathematics, Washington University, St. Louis, MO 63130, USA
†Dept. of Chemical Engineering, Washington University, St. Louis, MO 63130, USA

Among the fundamental assumptions Knudsen makes in his theoretical considerations is that the direction in which a molecule rebounds from a solid wall is independent of the direction in which it approaches the wall and is governed by the *cosine law*: the probability ds that a molecule leaves the surface in the solid angle $d\omega$ forming an angle θ with the normal to the surface (Figure 1) is

$$ds = \frac{d\omega}{\pi} \cos\theta. \tag{1}$$

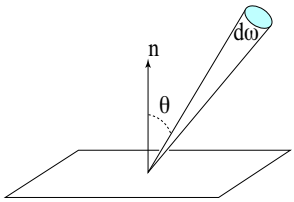

Figure 1. $d\omega$ is the solid angle in the expression of the cosine law. The distribution of scattered velocities is independent of the incidence angle.

Using this assumption he derives a theoretical result about gas flow through tubes that is in very good agreement with his experimental data. [Kn, p.21-23]. Furthermore, he obtains direct experimental data that confirms the validity of the cosine law. [Kn, p.26-29].

The theoretical basis for the cosine distribution of velocities, however, remained unclear to him. It is interesting to read Knudsen's attempt to understand it ([Kn, p. 26]) and his dissatisfaction with his own explanations:

"To explain this I formed two hypothesis. In the one of them I assumed that the gas formed an adsorbed layer on the inner surface of the glass tube. If such a layer is sufficiently thick and dense the cosine law is readily explained. Against this hypothesis it may be said that the density of the adsorbed layer probably must increase with increasing pressure of the gas, and if so the molecules in the layer must be moving through the tube and may possibly cause the flow of gas to be stronger than the calculated molecular flow. In the other hypothesis I regarded the surface of the glass to be exceedingly rough so that an impinging gas molecule penetrated so deeply into the glass that by reason of its many collisions it forgot the direction in which it had approached the glass surface. I regarded the approaching molecule as a tennis ball falling to the ground through a wood with trees having many branches. Neither of these hypotheses nor a combination of them seemed very convincing to me, and they seemed still less convincing when I had proved that the energy-exchange between the impinging molecule and the glass surface may be very far from being complete. It is in fact very hard to understand that a collision between say a very fast moving hydrogen molecule and a glass surface should affect the magnitude of the molecular velocity but slightly and at the same time should alter the direction of the velocity completely."

More detailed molecular beam experiments later showed deviations from the cosine law, although it continues to be widely used as a fundamental assumption about gas scattering on weakly adsorbing surfaces. One of the simplest and

most frequently used refinements of the cosine law, described already by J.C. Maxwell, assumes that only a fraction α of the impinging molecules leave the wall according to the cosine law and that the remaining $1 - \alpha$ are specularly reflected. Maxwell's model has been extensively used, although it was felt to be somehow inadequate to represent experimental data and more complicated models were later proposed [CeSa, p. 32].

Therefore the following general questions naturally arise:

- Under what conditions, and to what degree, is the cosine law valid?
- What do deviations from it tell us about the gas-surface interaction?
- How does it relate to surface "roughness"?
- How do deviations from it affect diffusivity?

We wish to understand, by means of a concrete idealized model of gas-surface interaction, the precise nature and domain of validity of the cosine law. Our model is based on the notion of a billiard system with a geometric microstructure. It is essentially a geometric model and makes no ad-hoc assumptions about the stochastic properties of the interaction. Once the precise meaning of the term 'geometric microstructure' is clarified, the interaction will amount to ordinary billiard-ball type collision: gas molecules move freely inside a region of space until they collide elastically with a boundary surface and instantaneously rebound according to the usual law of equal angles of incidence and reflection.

Our theoretical model can be roughly described as follows. Geometric irregularities of the boundary surface, such as its varying curvature, naturally make the angle of reflection sensitive to the precise point at which a collision takes place. If, in a thought experiment, the size of these irregularities is scaled down by a similarity transformation (homothety), this sensitivity becomes more pronounced the smaller we choose the magnitude of reduction. At the limit, as this reduction factor approaches 0, the deterministic but highly unstable angle of reflection becomes effectively random. Its probability law, however, is still a function of the (scale independent characteristics of the) surface geometry. This asymptotic behavior is incorporated in the definition of a certain type of random dynamical system that will be referred to as a *random billiard* (with a given microgeometry). The details are given later in the paper.

The cosine law will be shown to arise as a stationary distribution for a Markov process associated to the random billiard. For a variety of microgeometries that are explored numerically, this distribution appears to be the unique stationary probability law, although one example is given for which the numerically stable distribution is a different one. Furthermore, in those cases where the stationary distribution indeed corresponds to the cosine law, the relaxation time will be shown, numerically, to vary greatly for different microstructures.

It is interesting to remark how the probabilistic character of the random billiard interaction model ultimately arises. The probabilistic behavior of a physical system often results due to some law of large numbers, in which a characteristic number, μ, is passed to the limit, $\mu \to \infty$. Typically, it is the

number of molecules or an interval of time. In the present case the characteristic parameter is the ratio λ_1/λ_2, where λ_1 is the mean free path, which in the Knudsen regime can be taken to be a characteristic length of the container or channel, and λ_2 is some characteristic length of the microscopic geometry of the boundary surface.

In this respect, probabilistic behavior is the result of combining two deterministic processes that exist at widely separated length scales: the free motion at lengths comparable to λ_1 and the microscopic billiard motion at lengths comparable to λ_2. (A parameter that can be used experimentally to establish a link between these two scales is the actual diameter of the gas molecules. We will explain and make use of this simple remark in a forthcoming paper.)

That only two length scales are distinguished in our analysis is a simplifying assumption and not a fundamental limitation of the approach. What is important is that the structure of the solid surface is defined by a hierarchy of geometries with characteristic lengths $\lambda_1 > \lambda_2 > \cdots$, where each λ_i can be regarded as the mean free path of a point particle at the respective scale and, for each i, λ_{i+1} is assumed much smaller than λ_i. (Although the billiard particles are described above as point-like, the analysis does take into account the molecular diameter, as will be seen later. It will be apparent then that the smallest scale of interest is limited by the size of the gas molecules, thereby precluding true fractal geometries. Clearly, specular reflection off a fractal surface does not make sense as these surfaces do not admit normal vectors.)

Since most of our study will be carried out for only two scales, a convenient way to distinguish them in the text is to append the prefixes 'macro' and 'micro' to certain terms. Consider, for example, the term 'collision'. It is implicit in the definition of λ_i that collision between molecule and surface should also be understood hierarchically and that λ_2 is within the margin of error that specifies the *accuracy* with which λ_1 is measured. Thus 'macrocollision' will refer to a collision that can be regarded as a unitary process for a given accurancy, i.e., that cannot be resolved into more elementary collisions at that accuracy, but may consist of a number of microcollisions happening in close succession at a site on the surface of diameter comparable to λ_2.

Here is a brief outline of the paper. Section 2 contains a brief discussion of the model of gas-surface interaction that is most commonly used in the literature. The fundamental concept of a *scattering kernel* is reviewed there and its main properties are recalled.

The random billiard model is explained in Section 3. It is shown in Section 4 that the scattering kernel of a random billiard satisfies the fundamental property of *reciprocity*. In essence, this property states that the distribution of velocities specified by the cosine law is not changed by the scattering operator. This is interpreted in Section 5 in terms of stationary distributions for a Markov process associated to the scattering operator.

It is shown in Section 6 that the random billiard model is a limit of a family of deterministic billiard-type systems when the length scale of the microgeometry approaches 0. This implies that the main probabilistic assumption of the model is both necessary and natural.

Section 7 illustrates the main conclusions with a number of numerical examples. These include a geometry with fast convergence to the cosine law, another with slow convergence, as well as an example that does not admit the cosine law as a numerically stable distribution. We also exhibit a family of examples in which a simple geometry is probed by spherical molecules of varying radii. An important feature of the gas-solid interaction model we adopt is that it is sufficiently simple and explicit to be approached by molecular dynamics simulation, and flexible enough to allow for a great variety of interaction properties. More sophisticated geometric models (as in [MaCo, Co], for example) can be devised, but a systematic, first-principles analysis of the type we seek would be rather difficult for them.

We lay here the groundwork for a study of Knudsen flow that we plan to continue in a second paper. The final goal is to relate macroscopic properties of the gas transport in channels, such as diffusivity constants, with microscopic features of the channel's surface. This relationship will be explored in the context of TAP-experiments (*Temporal Analysis of Products*), an experimental technique pioneered by J. Gleaves, which has been extensively used by Gleaves, Yablonsky and others to investigate heterogeneous catalysis. [GEK, GYPS, YOM]. In the follow-up paper a TAP experiment will be numerically run for a family of random billiards specified by a set of geometric parameters, and the influence of the microgeometry on the time characteristics of the flow will be investigated.

2 The Standard Model of Knudsen Flow

The stochastic model of molecular flow in the Knudsen regime, as it is commonly described in the literature, is briefly summarized here so that the model to be proposed later can be placed in proper perspective. A good reference for this material is [Ce], or [CeSa].

We first define a few general terms. Let C be a region in space whose boundary is the union of a finite number of smooth surfaces. The unit normal vector, directed inward, at a point $\mathbf{x}$ on the boundary is denoted by $\mathbf{n}(\mathbf{x})$. C will often be a 2-dimensional region, in which case it is understood that the boundary is a collection of smooth curves. C is referred to as the *channel*. Some of the boundary component surfaces are regarded as part of C and called *walls*. The other components are the *open sides* of the channel. For example, if C is a solid cylinder of finite length the (single) wall is a cylindrical surface and the open sides are the two discs at the opposite ends.

A *gas* in C consists of a large number of point-like particles that undergo free motion in the interior of C and interact with the surface in a way to be specified shortly. In the continuous approximation, the state of the gas is specified by a one-particle probability density, or distribution function $f(\mathbf{x}, \mathbf{u}, t)$, where t is time, $\mathbf{x}$ is the position in C and $\mathbf{u}$ is the velocity. As it will not matter which normalization is used, this function may also be interpreted as a mass density function. Thus, denoting by $d\mathbf{x}d\mathbf{u}$ the volume of a small region in the position-velocity space containing $(\mathbf{x}, \mathbf{u})$, $f(\mathbf{x}, \mathbf{u}, t)d\mathbf{x}d\mathbf{u}$ is the mass of all molecules of

the gas for which the position and velocity lie in that region at time t.

In the Knudsen regime approximation it is supposed that the gas is sufficiently rarefied for collisions between molecules to be negligible. The characteristic properties of collisions between molecules and the wall are specified probabilistically by a *scattering kernel*, $R(\mathbf{u} \to \mathbf{u}'; \mathbf{x}, t, \tau)$. This is the probability density function for the event that, after hitting the wall at $\mathbf{x}$ with velocity $\mathbf{u}$, where $\mathbf{u} \cdot \mathbf{n}(\mathbf{x}) < 0$, a molecule will reemerge a time τ later with velocity $\mathbf{u}'$, $\mathbf{u}' \cdot \mathbf{n}(\mathbf{x}) > 0$, at approximately the same $\mathbf{x}$.

When the adsorption time of molecules impinging on the wall is negligible compared to any characteristic time of interest, it is more convenient to work with the density defined by

$$R(\mathbf{u} \to \mathbf{u}'; \mathbf{x}, t) = \int_0^\infty R(\mathbf{u} \to \mathbf{u}'; \mathbf{x}, t, \tau) d\tau. \tag{2}$$

The molecular flow in C is described by the linear Boltzmann equation:

$$\frac{\partial f}{\partial t} + \mathbf{u} \cdot \nabla_{\mathbf{x}} f = 0, \tag{3}$$

where $\nabla_{\mathbf{x}} f = (\frac{\partial f}{\partial x}, \frac{\partial f}{\partial y}, \frac{\partial f}{\partial z})$. To Equation 3 the following boundary condition must be added: on the open sides it is assumed that $f = 0$, and on the channel walls

$$f(\mathbf{x}, \mathbf{u}, t)|\mathbf{u} \cdot \mathbf{n}| = \int_0^\infty \left(\int_{\mathbf{v} \cdot \mathbf{n} < 0} f(\mathbf{x}, \mathbf{v}, t - \tau) R(\mathbf{v} \to \mathbf{u}; \mathbf{x}, t, \tau) |\mathbf{v} \cdot \mathbf{n}| d\mathbf{v} \right) d\tau, \tag{4}$$

for all $(\mathbf{x}, \mathbf{u})$ such that $\mathbf{u} \cdot \mathbf{n} > 0$, where $\mathbf{n} = \mathbf{n}(\mathbf{x})$. (See [CeSa], equation 1.10.4, p. 29.)

Equation 3 and boundary condition 4 express the hypothesis that molecules move freely between collisions with the wall and, after collisions, they scatter according to R. This boundary value problem will be approached numerically, in a subsequent paper, by direct simulation of the molecular random walk along the channel specified by a choice of scattering kernel. For much of the present paper our focus is on the scattering kernel R itself, and the associated scattering operator to be introduced shortly.

The simplest choice of scattering kernel, which is essentially Knudsen's cosine law (at temperature T), is

$$R_{\text{Knud}}(\mathbf{u} \to \mathbf{u}') = M(\mathbf{u}')|\mathbf{u}' \cdot \mathbf{n}| \tag{5}$$

where $M(\mathbf{u}') = \frac{2\beta^2}{\pi} e^{-\beta|\mathbf{u}'|^2}$ is the (non-drifting) Maxwellian distribution of velocities and $\beta = m/2RT$.

Purely specular reflection off a smooth surface corresponds to the kernel

$$R_{\text{spec}}(\mathbf{u} \to \mathbf{u}') = \delta(\mathbf{u}' - \mathbf{u} + 2(\mathbf{u} \cdot \mathbf{n})\mathbf{n}) \tag{6}$$

where $\delta(\mathbf{w})$ is the Dirac delta function concentrated at $\mathbf{w}$.

Another widely used kernel is the so called *Maxwell's model*. In this case a molecule impinging on the surface undergoes, with probability α, specular reflection, and with probability $1-\alpha$ it is diffusely reflected with a non-drifting Maxwellian distribution of velocities; i.e.,

$$R = \alpha R_{\text{spec}} + (1-\alpha) R_{\text{Knud}}. \tag{7}$$

The systematic study of scattering kernels began at the end of 1960's. This study suggests that for most gas-surface interactions R should have the following fundamental properties:

1. *Non-negativity.* $R(\mathbf{u} \to \mathbf{u}'; \mathbf{x}, t, \tau) \geq 0$;

2. *Normalization.* If permanent adsorption is excluded, then

$$\int_0^\infty \int_{\mathbf{v}\cdot\mathbf{n}<0} R(\mathbf{u} \to \mathbf{v}; \mathbf{x}, t, \tau) d\mathbf{v} d\tau = 1; \tag{8}$$

3. *Reciprocity.* For $\mathbf{u}\cdot\mathbf{n} < 0$, $\mathbf{u}'\cdot\mathbf{n} > 0$,

$$\frac{R(\mathbf{u} \to \mathbf{u}'; \mathbf{x}, t, \tau)}{R_{\text{Knud}}(\mathbf{u} \to \mathbf{u}')} = \frac{R(-\mathbf{u}' \to -\mathbf{u}; \mathbf{x}, t, \tau)}{R_{\text{Knud}}(-\mathbf{u}' \to -\mathbf{u})}. \tag{9}$$

Reciprocity is "a subtler property that follows from the circumstance that the microscopic dynamics is time reversible and the wall is assumed to be in a local equilibrium state, not significantly disturbed by the impinging molecule." [CeSa, p. 30]. It implies (by integration) that $M(\mathbf{u})|\mathbf{u}\cdot\mathbf{n}|$ is a fixed point of the integral operator with kernel R. In other words,

$$M(\mathbf{u})|\mathbf{u}\cdot\mathbf{n}| = \int_{\mathbf{u}'\cdot\mathbf{n}<0} R(\mathbf{u}' \to \mathbf{u}; \mathbf{x}, t) M(\mathbf{u}')|\mathbf{u}'\cdot\mathbf{n}| d\mathbf{u}'. \tag{10}$$

If collisions do not alter the kinetic energy of molecules (which is the case in the billiard model we adopt later), then Equation 10 readily implies that Knudsen's cosine law is a fixed probability distribution for the scattering operator.

We emphasize that the gas transport in our study is governed by the above boundary value problem and not, a priori, by a diffusion equation. The latter, when valid, is an approximation due to the central limit theorem. For example, if C is a cylinder, then under an appropriate scaling limit (for small radius) Equation 3 has a diffusion limit, as shown in [Ba]. The corresponding problem in dimension 2, or for two parallel plates in dimension 3, requires very different rescaling to produce a diffusion limit, and the resulting process has rather exceptional properties. See, for example, [BGT].

3 The Random Billiard Model

Our statistical model of gas-surface interaction is derived from a *billiard dynamical system* model for the elementary collisions between molecule and wall channel. Two points should be emphasized:

- We regard the Hamiltonian (non-dissipative) interaction between gas and wall surface as purely geometric, that is, as a billiard ball (hard sphere model) collision.
- Knudsen's cosine law should be understood on the basis of this deterministic dynamics, with as few *ad hoc* probabilistic assumptions as possible.

Before describing the model in greater detail it is natural to ask whether a hard spheres model is justified. As noted in [ArChMa], "[p]revious work on diffusion in nanopores [...] has shown that the thermalization time of the sorbate molecule with the surrounding lattice is often much larger than the collision time for the case of weakly adsorbing molecules with kinetic diameters much less than half the pore width. For these situations, lattice vibrations are relatively unimportant and little stochastic thermal force exists during each wall collision event. Instead, the stochastic forcing is due to the chaotic Hamiltonian and deterministic trajectory of the constant-energy molecule in the pore." (See references cited in [ArChMa].)

3.1 General Description of the Model

The key idea is summarized in Figure 2.

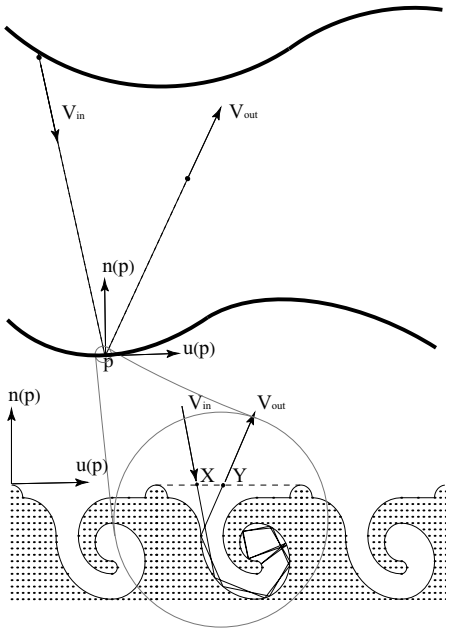

Figure 2. The random billiard system with (a somewhat fanciful) microgeometry. For a $\mathbf{V}_{\text{in}}$ determined by the outcome of the previous (macro-) collision and a random point $\mathbf{X}$ chosen with uniform probability distribution over a period of the microgeometry (the dotted line segment over the microcage), the velocity $\mathbf{V}_{\text{out}}$ is obtained by following the billiard-ball motion inside the microcage.

Notice that the model distinguishes two scales: the macroscale of the channel and the microscale at which the regular array of "billiard tables" shown at the bottom of the picture becomes apparent. Our main concern in this paper is with what happens at the microscale level, as we change the shape of these billiard tables. The channel walls are represented by the thick solid lines. The figure describes a single macrocollision at a point $\mathbf{p}$ on the lower side of the wall, consisting of several microcollisions of specular type. Although not strictly necessary, we consider *periodic* microgeometries. The dotted line segment on the lower part of the figure represents a single period of this lattice-like structure. In three dimensions this lattice element is a two-dimensional piece of plane which we refer to as a *cell* and denote by $\mathcal{O}$. As the mean free path between two macrocollisions is much greater than the size of the cell, it can be assumed that the exact point of incidence is a random variable uniformly distributed over $\mathcal{O}$. (This is further explained in section 6.)

The *scattering kernel*, $R(\mathbf{V}_{\text{in}} \to \mathbf{V}_{\text{out}}; \mathbf{p})$, is now obtained by the following procedure. The billiard motion at the microscale specifies a canonical (Hamiltonian) map $(\mathbf{X}, \mathbf{V}_{\text{in}}) \to (\mathbf{Y}, \mathbf{V}_{\text{out}})$, where $\mathbf{X}$ and $\mathbf{Y}$ lie in $\mathcal{O}$ and $\mathbf{V}_{\text{in}} \cdot \mathbf{n} < 0$, $\mathbf{V}_{\text{out}} \cdot \mathbf{n} > 0$. This gives a deterministic function

$$\mathbf{V}_{\text{out}} = \mathbf{V}(\mathbf{X}, \mathbf{V}_{\text{in}}) \tag{11}$$

We now regard $\mathbf{X}$ as a random variable uniformly distributed over $\mathcal{O}$, making $\mathbf{V}_{\text{out}}$ a random function of $\mathbf{V}_{\text{in}}$. The probability density of this random function is the scattering kernel.

3.2 Mathematical Refinements

The above description should suffice for the later sections of the paper. In the rest of this section we elaborate on a few mathematical points needed for later justifying some of the claims made earlier. This requires first introducing a bit of notation. We simplify the discussion by supposing that the lattice cell of the microgeometry is rectangular. (A rectangle with periodic "boundary condition" is a 2-*torus*.)

A periodic microgeometry is a parametric surface defined by a vector valued function $\mathbf{F}(x, y) = F_1(x, y)\mathbf{i} + F_2(x, y)\mathbf{j} + F_3(x, y)\mathbf{k}$ such that

$$\mathbf{F}(x + m, y + n) = \mathbf{F}(x, y) + m\mathbf{i} + n\mathbf{j}, \tag{12}$$

where m, n are arbitrary integers. It is convenient to assume that the maximum value of F_3 is 0. Therefore the surface lies between, and touches, the parallel planes: $z = 0$ and $z = -h$, where h is the height of the surface. $\mathbf{F}$ divides 3-space in two regions. The region containing the points with positive z-coordinate will be referred to as the *interior* region. This is the white region in Figure 3. (The particular microgeometry of figure 3 is taken up later in the paper in our numerical study as an example of a very "dispersive" billiard system.)

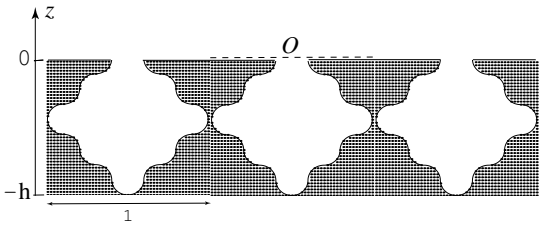

Figure 3. An example of a 2-dimensional microgeometry. F is the boundary line of the shaded area and $\mathcal{O}$ is the top line segment over a period of F. Observe that $\mathcal{O}$ is bigger than the mouth of the microcavity by a factor of 5. This example will be referred to later as the *wavy geometry*.

We also assume that for all points $\mathbf{x} = (x, y, z)$ on the surface, except possibly over a set of 0-area, a normal vector $\mathbf{n}_{\text{mic}}(\mathbf{x})$ directed to the interior region is defined and is continuous. This will be called the *micronormal* vector to the surface, to distinguish it from the (*macro-*) normal vector field defined earlier for the surface of the channel. The surface $\mathbf{F}$ over a single period is the boundary of a three-dimensional *billiard table.* In Figure 3, for example, the table is any one of the open cavities.

The above defines the main geometric data of the model. It should be noted that the length scale of the microgeometry is not relevant; the "actual" surface geometry will be defined by "superposing" $\mathbf{F}$ to a flat surface at a given length scale to be specified by some additional parameter, a, which is taken later as the diameter of the gas molecules. The periodicity of $\mathbf{F}$ is a convenient hypothesis which can be greatly relaxed.

3.3 Obtaining the Scattering Kernel

From now on, we use lower-case letters, such as $\mathbf{x}$ and $\mathbf{v}$, to denote specific points and velocities and reserve the upper-case letters, $\mathbf{X}$ and $\mathbf{V}$, for the corresponding random variables. This convention applies to position and velocity variables only.

The *phase space* of the open billiard is the set of all pairs $(\mathbf{x}, \mathbf{v})$, where $\mathbf{x} \in \mathcal{O}$ and $\mathbf{v}$ is a vector. When $\mathbf{v} \cdot \mathbf{k} < 0$ (resp., $\mathbf{v} \cdot \mathbf{k} > 0$), $\mathbf{v}$ represents the velocity of an incoming (resp., outgoing) particle.

The *billiard transformation* is a mapping $T(\mathbf{x}, \mathbf{v}) = (\mathbf{y}, \mathbf{w})$ defined as follows. An incoming point particle with initial condition $(\mathbf{x}, \mathbf{v})$ undergoes ordinary billiard ball motion inside the cavity until it returns to the open side. The point of return is then $\mathbf{y}$ and the new velocity is $\mathbf{w}$. Clearly, $\|\mathbf{v}\| = \|\mathbf{w}\|$; a collision at $\mathbf{x}$ on the boundary surface of the billiard table changes the particle's velocity according to $\mathbf{u} \to \mathbf{u} - 2\mathbf{u} \cdot \mathbf{n}_{\text{mic}}(\mathbf{x})\mathbf{n}_{\text{mic}}(\mathbf{x})$.

For all initial conditions representing an incoming particle except, possibly, for a set of volume 0 in phase space, the particle eventually returns to the open side. (This is a direct consequence of the *Poincaré recurrence theorem*, a basic result in the theory of dynamical systems. See, for example, [HK]. It is

possible for certain geometries, even in dimension 2, that an incoming particle with very special initial conditions can become trapped in the open cavity and never again escape. However, the initial conditions for such events constitute a set of measure 0 with respect to the Liouville measure on the phase space of the billiard system.) Therefore, for an arbitrary surface $\mathbf{F}$ the map T makes sense, at least over a subset of full volume in phase space.

A molecule (point particle) moves freely in the interior of the channel until it impinges on a point $\mathbf{p}$ on the wall with velocity $\mathbf{v}_{\text{in}}$. From that point it emerges with velocity $\mathbf{V}_{\text{out}}$ having the same speed and random direction defined by a scattering kernel, whose precise description can now be given. After an appropriate rotation of coordinates we regard $\mathbf{k} = \mathbf{n}(\mathbf{p})$. Let $\mathbf{X}$ be a random point on $\mathcal{O}$ with constant probability density; then $\mathbf{V}_{\text{out}}$ is the random function obtained by means of the equation

$$T(\mathbf{X}, \mathbf{v}_{\text{in}}) = (\mathbf{Y}, \mathbf{V}_{\text{out}}). \tag{13}$$

We now define $R(\mathbf{v}_{\text{in}} \to \mathbf{v}_{\text{out}})$ as the probability density of $\mathbf{V}_{\text{out}}$.

3.4 First Example

Figure 5 shows the graph of the scattering kernel for the *zig-zag geometry*, which is defined at the bottom of the picture. It consists of a see-saw function of right-triangles. The scattering kernel for this example is given as a function of the angles of incidence, θ_{in} , and reflection, θ_{out} . The angle convention is defined in Figure 4.

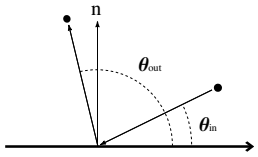

Figure 4. Angle convention for the scattering kernel in dimension 2.

The scattering kernel of the zig-zag geometry is a Dirac delta-like function supported on the figure H on the graph. This example shows that $\mathbf{V}_{\text{out}}$ may not have a proper density function. Its density exists in the sense of distributions, or generalized functions. Because of this, it may be more convenient at times to regard as the more fundamental quantity not R itself but the operator on measures of which R is the integral kernel.

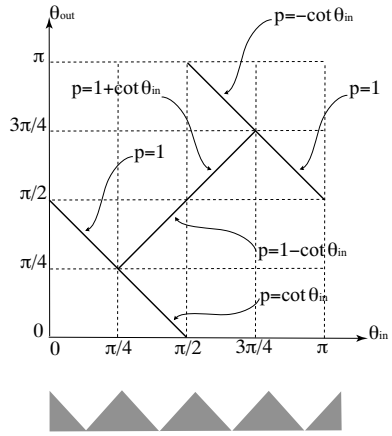

Figure 5. Scattering kernel for the zig-zag geometry. The angles θ_{in} and θ_{out} are measured as in figure 5. The graph should be interpreted as follows: If the angle of incidence is, say, between $\pi/4$ and $\pi/2$, then θ_{out} can take one of two values: θ_{in} or $\pi/2 - \theta_{\text{in}}$, with probabilities $1 - \cot(\theta_{\text{in}})$ and $\cot(\theta_{\text{in}})$, respectively.

3.5 The Scattering Operator Associated to R

It is convenient to define the *scattering operator*, $\mathcal{R}$, associated to a scattering kernel R. This is defined as follows. Let S^- denote the set of incoming directions, that is, the hemisphere consisting of unit vectors $\mathbf{u}$ such that $\mathbf{u} \cdot \mathbf{k} \leq 0$. Similarly define S^+. Let A be the ordinary area measure on $\mathcal{O}$, that is, $dA(\mathbf{x}) = dxdy$. We assume that the area of $\mathcal{O}$ is normalized to 1. Then, to any probability measure ν on S^-, the function $\mathbf{V}_{\text{out}}(\mathbf{x}, \mathbf{v}_{\text{in}})$ naturally associates a probability measure on the space of outgoing directions, which is described below. (An economic mathematical description is to say that the measure is the *push-forward* of the product measure $A \otimes \nu$, denoted $(\mathbf{V}_{\text{out}})_*(A \otimes \nu)$.) The resulting measure is by definition $\mathcal{R}(\nu)$ and we call $\mathcal{R}$ the scattering operator associated to the microgeometry $\mathbf{F}$. More explicitly, for any continuous function g on S^+, and any probability measure ν on S^-, the integral of f with respect to $\mu = \mathcal{R}(\nu)$ is given by

$$\int_{S^-} f(\mathbf{u}) d\mu(\mathbf{u}) = \int_{S^-} \int_{\mathcal{O}} f(\mathbf{V}_{\text{out}}(\mathbf{x}, \mathbf{v})) dA(\mathbf{x}) d\nu(\mathbf{v}). \tag{14}$$

3.6 Markov Chain Approximation

For the numerical examples investigated later in the paper, it will be necessary to approximate the scattering kernel by a Markov transition matrix. In dimension 2 this is done as follows. We represent $\mathbf{v}_{\text{in}}$ and $\mathbf{v}_{\text{out}}$ by the respective angles, as indicated in Figure 4. Let $\theta_{\text{out}} = \Theta(x, \theta_{\text{in}})$ be the function $\mathbf{v}_{\text{out}}$ of $(\mathbf{x}, \mathbf{v}_{\text{in}})$ written in terms of those angles. Let ν_{in} be a probability measure on $[0, \pi]$ defining a

distribution of incoming velocities and λ the ordinary length measure on the interval $[0, 1]$. We wish to describe a finite dimensional (matrix) approximation for $\mathcal{R}(\nu_{\text{in}})$.

Fix a partition of $[0, \pi]$ by intervals $I_1, I_2, \ldots, I_k$, and let $\theta_i \in I_i$ be a choice of representative angle for each I_i. Define a matrix (m_{ij}) whose entry m_{ij} is the measure of I_j assigned by $\mathcal{R}(\delta_{\theta_i})$. (Here δ_{θ_i} is the Dirac measure concentrated on θ_i.) In other words, if we define $\eta_i = \mathcal{R}(\delta_{\theta_i})$, then $m_{ij} = \int_{I_j} d\eta_i$. Thus m_{ij} is the probability that a particle with incoming angle θ_i reflects with angle in the interval I_j.

Figure 6 shows the finite state Markov process associated to a single initial angle, $\pi/3$, for the zig-zag geometry. An interpretation of this process is given later in the text. (See figure 9.)

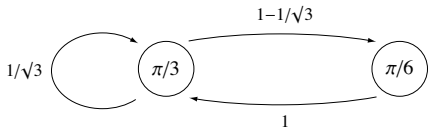

Figure 6. Markov chain associated to the initial value $\theta_{\text{in}} = \pi/3$, for the zig-zag geometry. This is obtained from Figure 5 by specializing the initial angle to $\pi/3$. The number inside each circle is a possible angle θ_{in} or θ_{out}. The numbers next to the arrows indicate the transition probabilities. An interpretation of the Markov process is given in Figure 9.

3.7 Non-zero Particle Diameter

Although we have assumed so far that our molecules are point-like particles, this is not an essential restriction. The important assumption is that the molecules are spherical and chemically inert. By following the motion of the center of mass we can regard the molecules as point particles while the wall microgeometry is "thickened" by an amount equal to the molecular radius as shown in Figure 7.

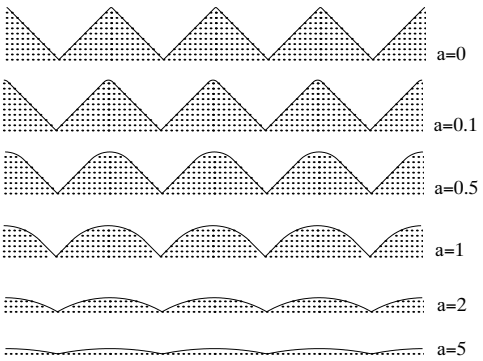

Figure 7. A wall contour (top, $a = 0$) is probed by molecules of varying radii. For each value of the radius, a, it is shown the center of mass view of the wall.

The figure describes a family of geometries that will be used later in numerical calculations. At the top of the picture is the actual relief of the wall while the contours with curved tops represent the center of mass view for molecules of different radii. The parameter a is the ratio of molecular radius by the height, h, of the top zig-zag contour. For large values of a the height of the corresponding contour is approximately $1/2a$.

4 Reciprocity

We wish to demonstrate here that the scattering operator associated to a random billiard satisfies the reciprocity condition. As noted in section 2, this is equivalent to the property that Knudsen's cosine law is a fixed probability measure for the scattering operator. More precisely, let η be the measure on S^- such that $d\eta(\mathbf{u}) = 2|\mathbf{u} \cdot \mathbf{k}|d\mathbf{u}$, where $d\mathbf{u}$ is the area element on the hemisphere. Then

$$\mathcal{R}(\eta) = \eta. \tag{15}$$

To see that Equation 15 indeed holds, consider the billiard system whose table is a cage of $\mathbf{F}$, which we close up by adding a flat lid on top. (Figure 8.) This is now an ordinary billiard table, without open sides. Consider the first return map to that flat side associated to the billiard transformation, which we denote by T.

T is a deterministic dynamical system with phase space $\mathcal{O} \times S^-$. (In dimension 2, the phase space is $[0,1] \times [0,\pi]$.) The billiard transformation has an invariant measure—the standard Liouville measure—given by $dL = dAd\eta$. (See [CFS].) In dimension 2 the measure is $\frac{1}{2}\sin\alpha dx d\alpha$, where α is the angle defined in the next picture.

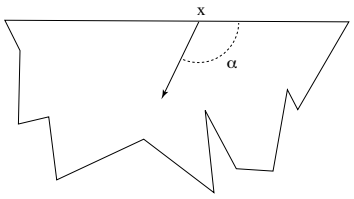

Figure 8. Billiard system obtained by closing up a cage with a flat lid.

Invariance of the Liouville measure under the return billiard transformation T means that, for any continuous function $f(\mathbf{x}, \mathbf{v})$ on $\mathcal{O} \times S^-$, the following equality holds:

$$\int_{S^-}\int_{\mathcal{O}} f(T(\mathbf{x},\mathbf{v}))dA(\mathbf{x})d\eta(\mathbf{v}) = \int_{S^-}\int_{\mathcal{O}} f(\mathbf{x},\mathbf{v})dA(\mathbf{x})d\eta(\mathbf{v}). \tag{16}$$

It follows immediately from this and the fact that $\mathcal{O}$ has area 1 that for every

continuous function h on S^-,

$$\int_{S^-}\int_{\mathcal{O}} h(\mathbf{V}_{\text{out}}(\mathbf{x},\mathbf{v}))dA(\mathbf{x})d\eta(\mathbf{v}) = \int_{S^-} h(\mathbf{v})d\eta(\mathbf{v}). \tag{17}$$

But the above is nothing but Equation 15, due to Equation 14.

5 Stationary Velocity Distributions

To discuss the validity of Knudsen's cosine law it is necessary to distinguish *single* and *multiple collision* scattering kernels. Our main observation can be summarized as follows:

- For a single molecule-wall collision the scattering kernel can deviate greatly from the cosine law;
- but for multiple collisions the law arises (for most, but not all, microgeometries) as an asymptotic probability distribution of post-collision scattering directions.

We give now a more detailed explanation of these points. It will be assumed that the channel is 2-dimensional, bounded by two parallel lines. Let $P_n(\theta_{\text{out}}|\theta_{\text{in}})$ denote the conditional probability density that a particle hitting the surface at an angle θ_{in} will, after an n-step random walk as indicated in Figure 9, emerge at an angle θ_{out}.

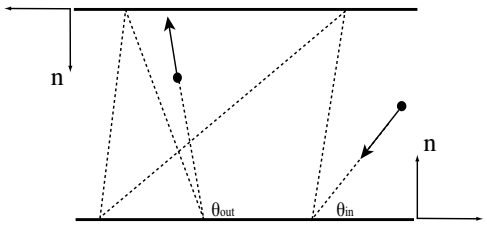

Figure 9. A 5-step random walk along the channel. The angles are measured counterclockwise from the horizontal axis. The conditional probability density that a particle will rebound at an angle θ_{out}, having hit the wall at an angle θ_{in} n-steps earlier is $P_n(\theta_{\text{out}}|\theta_{\text{in}})$.

P_n is the convolution (matrix multiplication in the finite dimensional approximation) of the scattering kernel with itself n-times. Some care is needed here to account for the way angles are measured, as the collisions alternate between the bottom and top boundary lines of the channel.

We reformulate Knudsen's cosine law as follows. (Due to the angle convention being used here we have a sine rather than cosine. Of course this is immaterial.)

For "most" microgeometries, $P_n(\theta_{out}|\theta_{in})$ converges to $\frac{1}{2}\sin\theta_{out}$ as $n \to \infty$, regardless of θ_{in}.

In other words, the cosine law should be understood as saying that Knudsen's probability distribution is a stable stationary probability for a Markov process associated to the scattering operator $\mathcal{R}$.

This cannot be true in all cases, as the trivial (flat) microgeometry immediately shows. (It is shown later that the zig-zag microgeometry is another counter-example.) The precise sense in which this reformulated Knudsen's law is expected to describe the asymptotic behavior of scattered velocities must be the subject of future work, in which 'most' will need to be replaced by geometric conditions on the microgeometry that are generic in some appropriate sense. A superficial explanation, however, can be given as follows. For Markov chains with finite state spaces there exists a unique stationary probability distribution if the chain is irreducible and aperiodic, that is, if for some positive integer k, all entries of M^k are positive, where M is a transition probability matrix obtained from a finite dimensional approximation of $\mathcal{R}$. (See, for example, [Wa].) Once a stationary measure is unique it follows that $M^n\mu$ will converge to it for an arbitrary initial probability vector μ.

It is natural to expect that most microgeometries will have enough dispersive scattering to ensure, after a sufficiently large number n of collisions, that every direction has a positive probability of following every other direction after n steps. (This, in any case, is strongly suggested by the numerical examples we have investigated, a few of which are shown later.) Since the measure with density $\sin\theta_{\text{out}}/2$ is always stationary as we saw earlier, it is the limit of P_n for the generic geometry.

The relaxation time of the Markov process can be fast or slow, depending on the type of microgeometry. This will be seen later in numerical examples. (In the examples, relaxation is taken as a function of the number of macrocollisions rather than time. The two quantities, however, are proportional on average.) We expect that this speed of convergence, properly defined to account for the initial distribution and macrogeometry of the channel, should provide a useful characteristic number for the microgeometry. Roughly, convergence is expected to be faster the more dispersive the scattering kernel is. (An appropriate theoretical framework in which these ideas is given in [Ru1].)

It is interesting to remark, in broad outline, how the cosine law for a random billiard system was obtained: the cosine distribution of velocities is an element of the description of a deterministic system, namely, the model billiard associated to the microgeometry $\mathbf{F}$, that survives the natural averaging process used to produce the scattering operator. We should observe, however, that in this section the "two-lines channel" geometry is used in an important way, not only for simplicity of visualization. The reason is that the relationship between the scattering operator and the Markov process explained here would be much more difficult to describe for, say, a cylinder, due to the dependence of $\mathbf{n}$ on the point on the wall of the channel. In the general case, the Markov process would involve iterating the scattering kernel followed by a random rotation. It is an interesting mathematical problem to show that for a generic geometry in 3-space η is still the unique stationary measure of scattered directions for the resulting random process. We will return to this problem in a future paper.

6 Random Limit of Deterministic Systems

We wish to explain here how the random billiard model arises as a limit of deterministic billiard systems. This is needed to justify our claim that the probabilistic assumption made in the definition of the scattering kernel (namely, that the point $\mathbf{X}$ in $\mathcal{O}$ is a random variable with constant probability density) is a necessary consequence of regarding the length scale of the surface microgeometry to be much smaller than the particle's mean free path inside the channel.

A precise way in which a random billiard is obtained from a family of deterministic billiards is explained here. (Since this will amount to convergence of measures in the weak*-topology, we call the result a *weak limit* of billiard systems.)

The microgeometry of a macroscopically smooth surface S is represented by a family of surfaces S_a converging to S when the scale parameter a approaches 0. Each S_a has model microgeometry defined by a common periodic surface $\mathbf{F}$. We regard S as an inner envelope for the family S_a. (See Figure 10.) The surface S_a converges pointwise to S from the outer side of S as $a \to 0$.

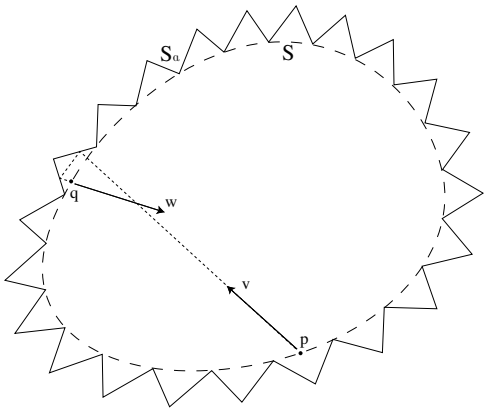

Figure 10. Approximation of the random billiard by a deterministic billiard at scale a. The limit surface S is the inner envelope of the approximating surface S_a.

Let $\mathbf{v}$ be the velocity at a point p on S. We follow the particle's trajectory from p until it collides with the surface at another point and reflects at a direction $\mathbf{w}$. Even though S_a converges to S as a set (in the so-called *Hausdorff topology*), clearly $\mathbf{w}$ may not converge to any definite limit.

A procedure that yields a well defined limit when $a \to 0$ is the following: as a first step, we replace $\mathbf{v}$ with a random variable $\mathbf{V}_\epsilon$ that is sharply concentrated around $\mathbf{v}$, and that approaches $\mathbf{v}$ with probability 1 when $\epsilon \to 0$. The scattered distribution for $\mathbf{V}_\epsilon$ is then obtained, resulting in a random variable with probability law $P_{a,\epsilon}$. We now pass the latter to the limit, first in a, giving the response of the system to a diffuse initial distribution of velocities, and finally in ϵ. Informally, the procedure corresponds to the idea that the microstructure

is supposed to be much smaller than any degree of accuracy which could in principle be used to specify the initial velocity $\mathbf{v}$.

More precisely, we begin by approximating $\mathbf{v}$ by a random variable with diffuse distribution concentrated near $\mathbf{v}$, that is, by a vector valued random variable having a continuous density $\rho^{\epsilon}_{\mathbf{v}}$ that converges to the Dirac delta function $\delta_{\mathbf{v}}$ as ϵ is sent to 0. The precise form of this density is immaterial.

Let now $\mu^{\epsilon}_{\mathbf{v},a}$ denote the resulting probability measure for outgoing velocities from S_a and incoming velocities with density $\rho^{\epsilon}_{\mathbf{v}}$. The scattering kernel for the limit random billiard will be shown to agree with the density of the weak*-limit $\mu_{\mathbf{v}}$ obtained in the following order:

$$\mu_{\mathbf{v}} = \lim_{\epsilon \to 0} \lim_{a \to 0} \mu^{\epsilon}_{\mathbf{v},a}. \tag{18}$$

If the microgeometry is flat, the resulting limit simply yields the ordinary, i.e., deterministic billiard system in the channel, C. In this case the scattering kernel is the delta function concentrated at the velocity of specular reflection.

For simplicity, these facts will be explained for 2-dimensional systems only. It will also be assumed that the (macro-) curvature of S is 0. These two assumptions will allow us to concentrate on the essential points that would otherwise be obscured by a number of mathematical technicalities. If the macroscopic curvature is not 0, it is nevertheless true that the surface line looks increasingly flat at smaller and smaller scales, so the outcome of the analysis would be the same as for a surface that is already flat and has the same model microgeometry.

Let $\mathbf{V}_a(\theta)$ be the outgoing velocity after collision with the line $\mathbf{F}_a$ for a particle that starts at the point $(0, 1)$ with velocity $\mathbf{v} = (\cos\theta\mathbf{i} - \sin\theta\mathbf{j})v$, where $0 < \theta < \pi$. (See Figure 11.) If T_a denotes the billiard map associated to $\mathbf{F}_a$, define $\mathbf{V}_a$ by:

$$T_a(a\{\cot\theta/a\}, \mathbf{v}(\theta)) = (y, \mathbf{V}_a(\theta)), \tag{19}$$

that is, $\mathbf{V}_a$ is the velocity component of $T_a(a\{\cot\theta/a\}, \mathbf{v})$, where $\{r\}$ denotes the fractional part of a number r. Notice that

$$T_a(a\{\cot\theta/a\}, \mathbf{v}) = T_1(\{\cot\theta/a\}, \mathbf{v}). \tag{20}$$

so $\mathbf{V}_a(a\{x/a\}, \mathbf{v}) = \mathbf{V}_1(\{x/a\}, \mathbf{v})$. The latter vector can also be represented by its angle measured counterclockwise from the horizontal axis: $\Theta(\{\cot\theta/a\}, \theta)$.

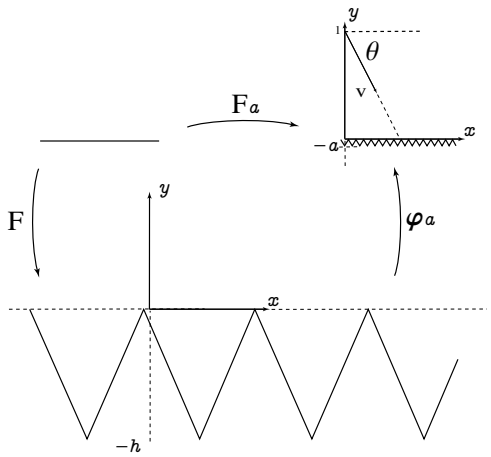

Figure 11. The model microgeometry is defined by the periodic (of period 1) parametric curve $\mathbf{F}(s) = (x(s), y(s))$. The actual boundary curve of the channel wall is $\mathbf{F}_a(s) = \varphi_a(F(s))$, where $\varphi_a(\mathbf{x}) = a\mathbf{x}/h$.

We can now give a more explicit description of the measure $\mu^{\epsilon}_{\mathbf{v},a}$ as follows: For any smooth function $g(\theta)$, $0 \le \theta \le \pi$, we define

$$\int_0^\pi g(\theta) d\mu^{\epsilon}_{\mathbf{v},a}(\theta) = \int_0^\pi g\left(\Theta\left(\left\{\frac{\cot\theta}{a}\right\}, \theta\right)\right) \rho^{\epsilon}_{\theta_0}(\theta) d\theta. \tag{21}$$

On the other hand, the probability measure defined by the random billiard, $\nu_{\mathbf{F}}$, associates to each smooth $g(\theta)$ the integral

$$\int_0^\pi g(\theta') d\nu_{\mathbf{v}}(\theta') = \int_0^1 g(\Theta(x,\theta)) dx, \tag{22}$$

where θ is the angle of $\mathbf{v}$. The density of $\nu_{\mathbf{v}}$ is the scattering kernel. (Strictly speaking, this density may exist only as a generalized function. The measure, however, is always defined.)

Therefore, our present goal is to show that for any smooth function $g(\theta)$ and for all θ and a outside of a set of zero measure, the following equality holds:

$$\lim_{a\to 0} \int_0^\pi g\left(\Theta\left(\left\{\frac{\cot\theta}{a}\right\}, \theta\right)\right) \rho^{\epsilon}_{\theta_0}(\theta) d\theta = \int_0^\pi \left(\int_0^1 g\left(\Theta\left(x,\theta\right)\right) dx\right) \rho^{\epsilon}_{\theta_0}(\theta) d\theta. \tag{23}$$

By taking $\rho^{\epsilon}_{\theta_0}$ sufficiently concentrated around θ_0, $0 < \theta_0 < \pi$, it can be supposed that the support of $\rho^{\epsilon}_{\theta_0}$ is contained in a closed interval in $(0, \pi)$. As to the function $\Theta(\{x\}, \theta)$, it is typically not continuous, but for a large class of billiard geometries $\Theta(\{x\}, \theta)$ is continuously differentiable on the complement of a closed set of total area 0 in the rectangle $[0,1] \times [0, \pi]$. See, for example, [KS]. In general it is not easy to characterize the exact degree of regularity of the map Θ, but it is not unduly restrictive on the possible billiard geometries

to suppose that $g\left(\Theta\left(\{x\},\theta\right)\right)$ can be replaced with its Fourier series in x and θ under the integrals of Equation 23.

Expanding $g(\Theta(\{x\},\theta))$ into Fourier series, it becomes apparent that Equation 23 is a consequence of the assertion:

$$\lim_{a\to 0}\int_0^\pi e^{2\pi i n\frac{\cot\theta}{a}} f(\theta)d\theta = 0 \tag{24}$$

for any $n \neq 0$ and any differentiable function $f(\theta)$ having compact support in $(0,\pi)$.

But limit (24) follows from facts about oscillatory integrals (method of stationary phase) and the fact that the derivative of $\cot\theta$ does not vanish on $(0,\pi)$. See, for example, [St].

7 Numerical Examples

We give a number of numerical examples in support of the main conclusions discussed above. The 3-dimensional "angle-in–angle-out–probability" diagrams shown below (figures 14-21) are graphs of the n-collision scattering kernel, P_n. They are all associated to two classes of microgemetries: the "wavy geometry" of figure 3 and the family of figure 7 for $a = 0, 0.1, 1$, and 5. In order to interpret them, recall that the scattering kernel and the P_n are functions of two variables, θ_{in} and θ_{out}. The pictures represent the graph of this function. The vertical axis parametrizes θ_{in}, the horizontal axis θ_{out} and the axis on the left hand side of the picture, which should be imagined as coming out of the plane of the page, gives the value of the function.

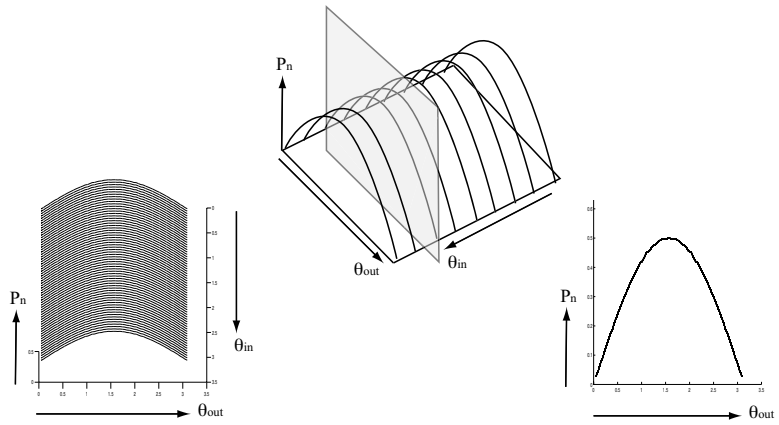

Figure 12. Interpretation of the graphs in figures 14-21. The graph on the right-hand side shows the superposition of the slices of the graph on the left for the sampled values of θ_{in}. The superposition is clear for figures 15 and 17 but for the bottom row of 19 (from which the above graphs are taken) it shows as a single line. Notice that the graph on the left is the same as that on top, only rotated to a different perspective.

The parameter δ is a crude measure of how far the distribution is from being stationary. More precisely, it measures the value of $\|(M-I)M^n\|/\|M^n\|$, where M is the Markov matrix approximation, and n is the number of collisions. The norm is defined as the maximum absolute value among the matrix entries.

The next graph summarizes the information about $-\log\delta$ as a function of $\log_2 n$. The values of n are those for which a graph of P_n is provided in one of the figures from 14 to 19.

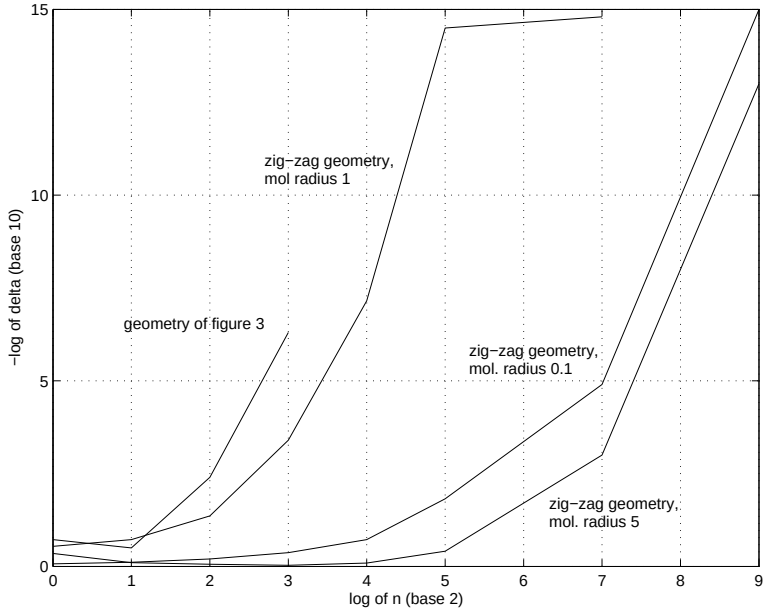

Figure 13. The bigger $-\log\delta$, the closer P_n is to the stationary distribution. Three of the above curves refer to the zig-zag geometry probed by molecules of different radii. The fourth refers to the "wavy geometry" of figure 3, section 3.

The first example shows very fast convergence to the cosine law. The microgeometry is the "wavy geometry" of figure 3 of section 3. It applies to the graphs on figures 14 to 17. Observe that in figure 3 the opening of the microcage is exactly 5 times the top length (i.e., the linear period of the microgeometry). Because of that, for about one step in every 5 the random walk falls into a cage and reemerges at a direction that is very sensitive to the position and velocity at the moment the particle entered it. We call this a *dispersive step* of the random walk. When the particle hits the flat top, it undergoes specular rebound, which does not change in any essential way the distribution of directions. We call the latter a *specular step*. For the graphs of P_n shown in figures 14 to 17 it is assumed that n only counts the number of dispersive steps. Therefore, actual convergence is about 5 times slower than the graphs might seem to indicate.

Figures 18 and 19 are associated to the family of figure 7. Recall that the parameter a is the ratio *molecular radius/depth of microgeometry*, where 'microgeometry' here refers to the zig-zag example. So for very small values of a, such as on the first (left) column of Figures 18 and 19, the effective microgeometry (i.e., as viewed by the molecule's center of mass) is very nearly the zig-zag one, for which relaxation is very

slow. (See figures 20 and 21.)

The second column, $a = 1$, is sufficiently dispersive to produce relatively fast relaxation. (We note, in passing, the similarity between the geometry of the graph $a = 1$ in figure 7 and the scatterer of Sinai dispersing billiards, which are well-known to have strongly stochastic properties.)

On the third column, the large value of a makes the effective microgeometry very nearly flat. (Figure 7, graph $a = 5$.) In this case, relaxation is again relatively slow.

The poor approximation to the sine function for large values of n in the lower left graph of Figure 19 is due to the limited precision with which angles were sampled in the Markov approximation of the scattering kernel. (Compare the top left graph of Figure 18 with Figure 20. For the latter, the sampling is 5 times finer.) That notwithstanding, we expect the cosine law to hold for all positive values of a.

The third example, for which a is exactly 0, is not sufficiently dispersive and converges rather slowly. Moreover, it converges to a distribution that is not the cosine law. The geometry is the zig-zag example of Figure 4. This corresponds to Figures 20 and 21.

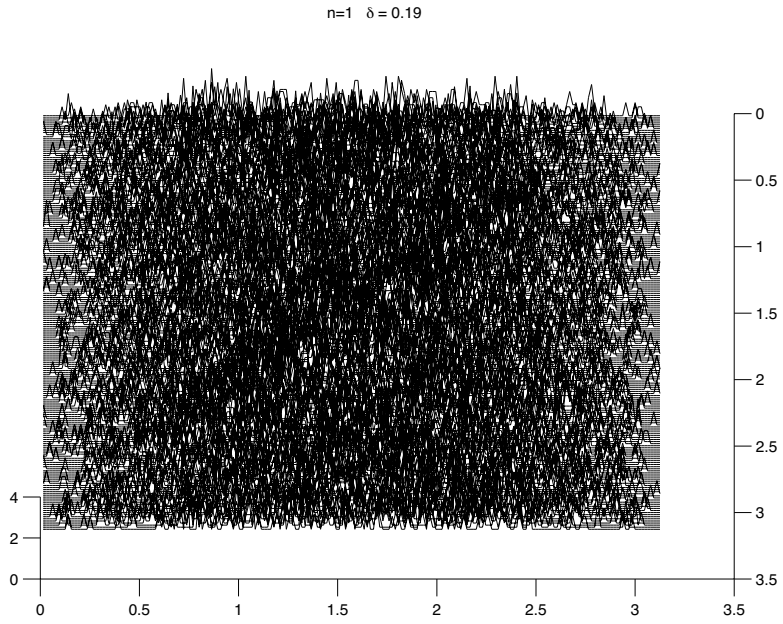

Figure 14. Graph of P_1.

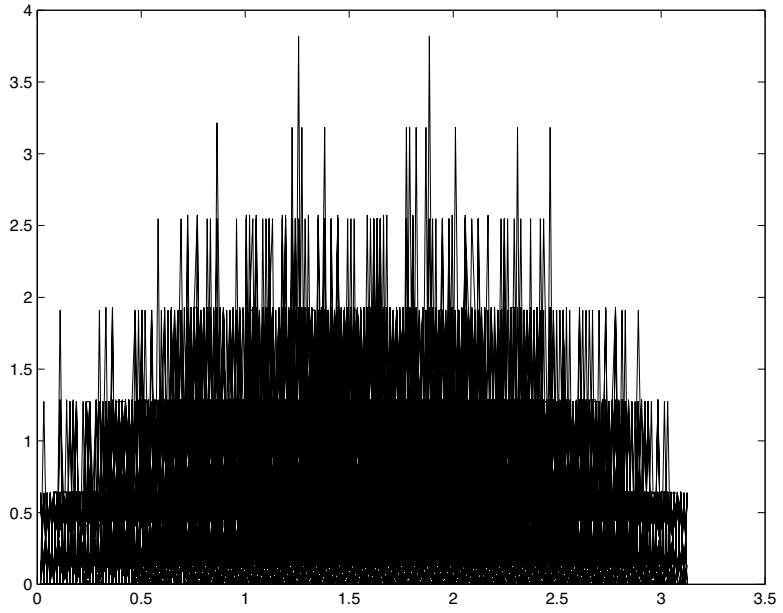

Figure 15. Same graph, in profile. Only the θ_{out} axis is visible.

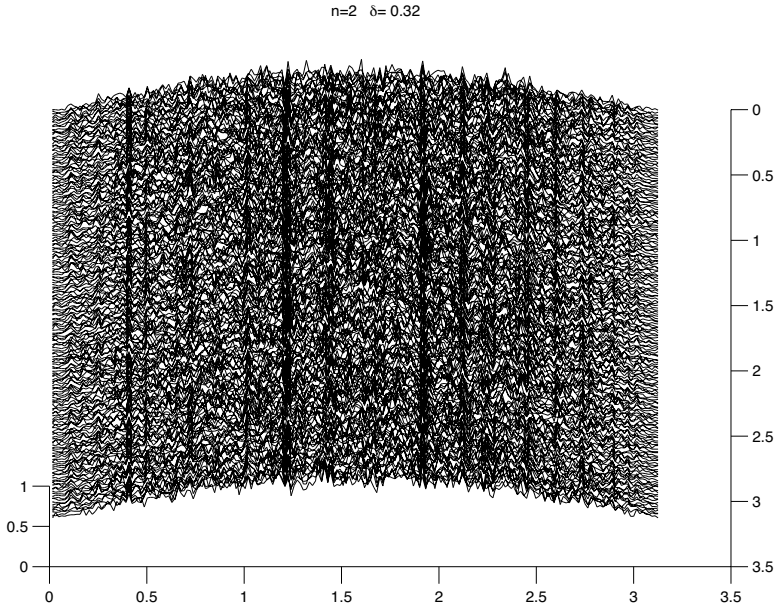

Figure 16. Graph of P_2.

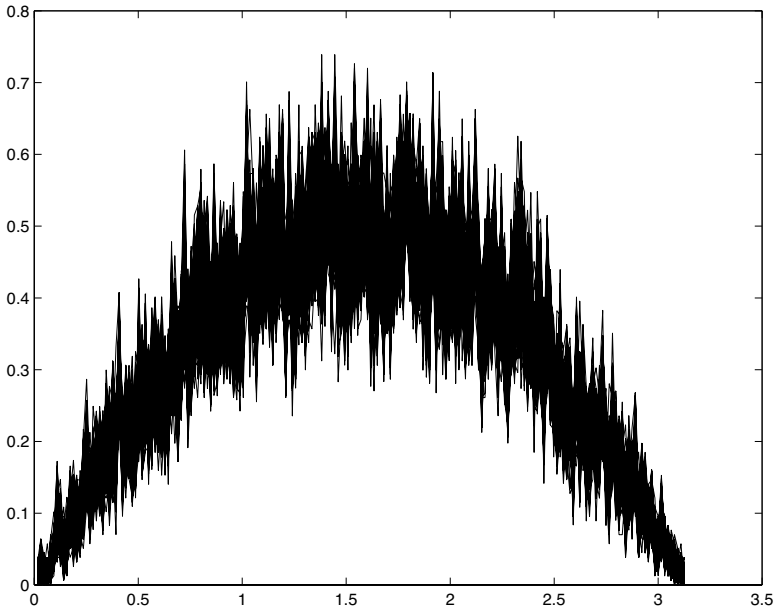

Figure 17. Graph of P_2 in profile.

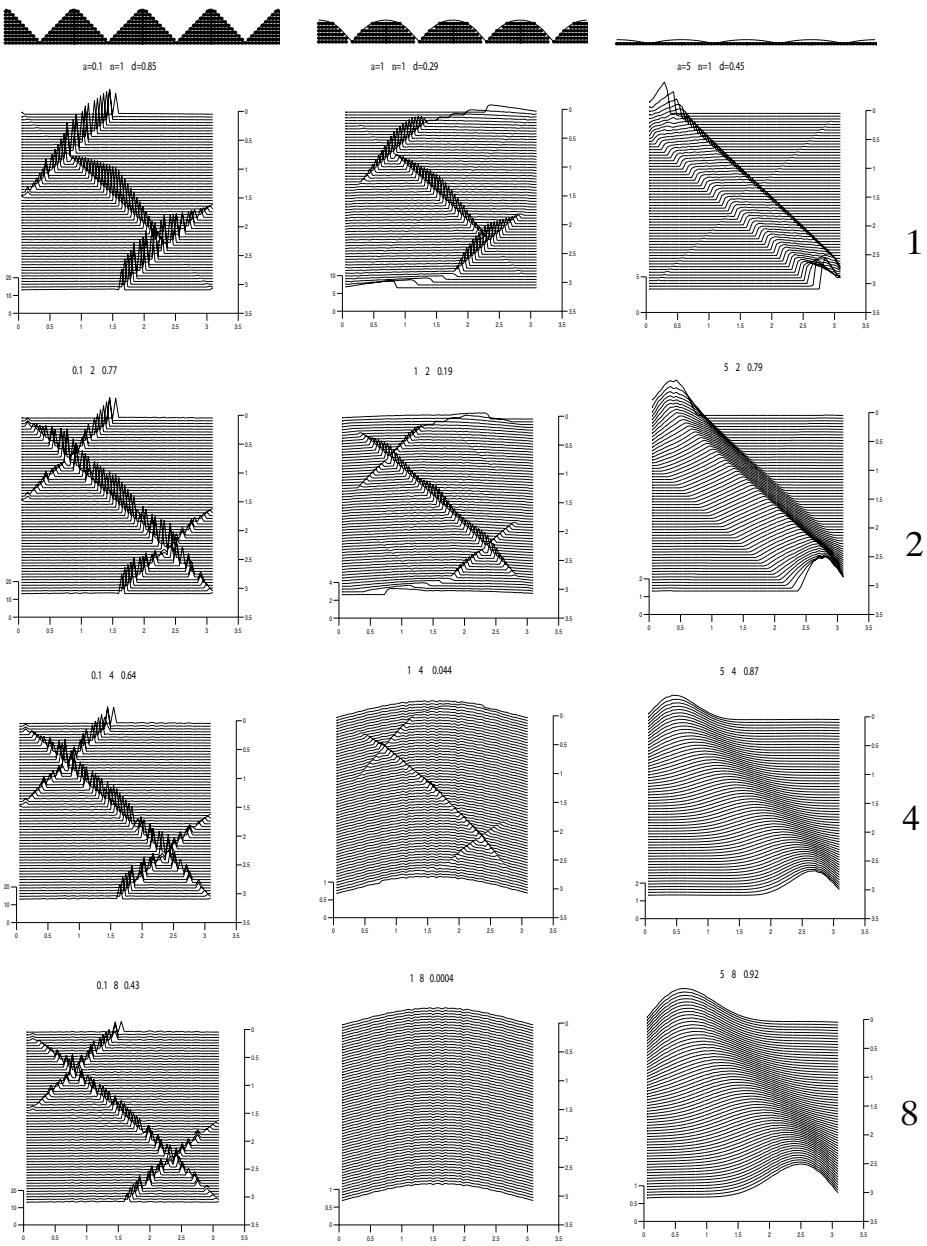

Figure 18. Graphs P_n for the family of Figure 3. The triple of numbers on top of each graph consists of the molecular radius, a, the number of collisions, n, and the distance to stationarity, δ. The microgeometry is indicated at the head of each of the three columns, and the number of collisions is shown to the right of each row.

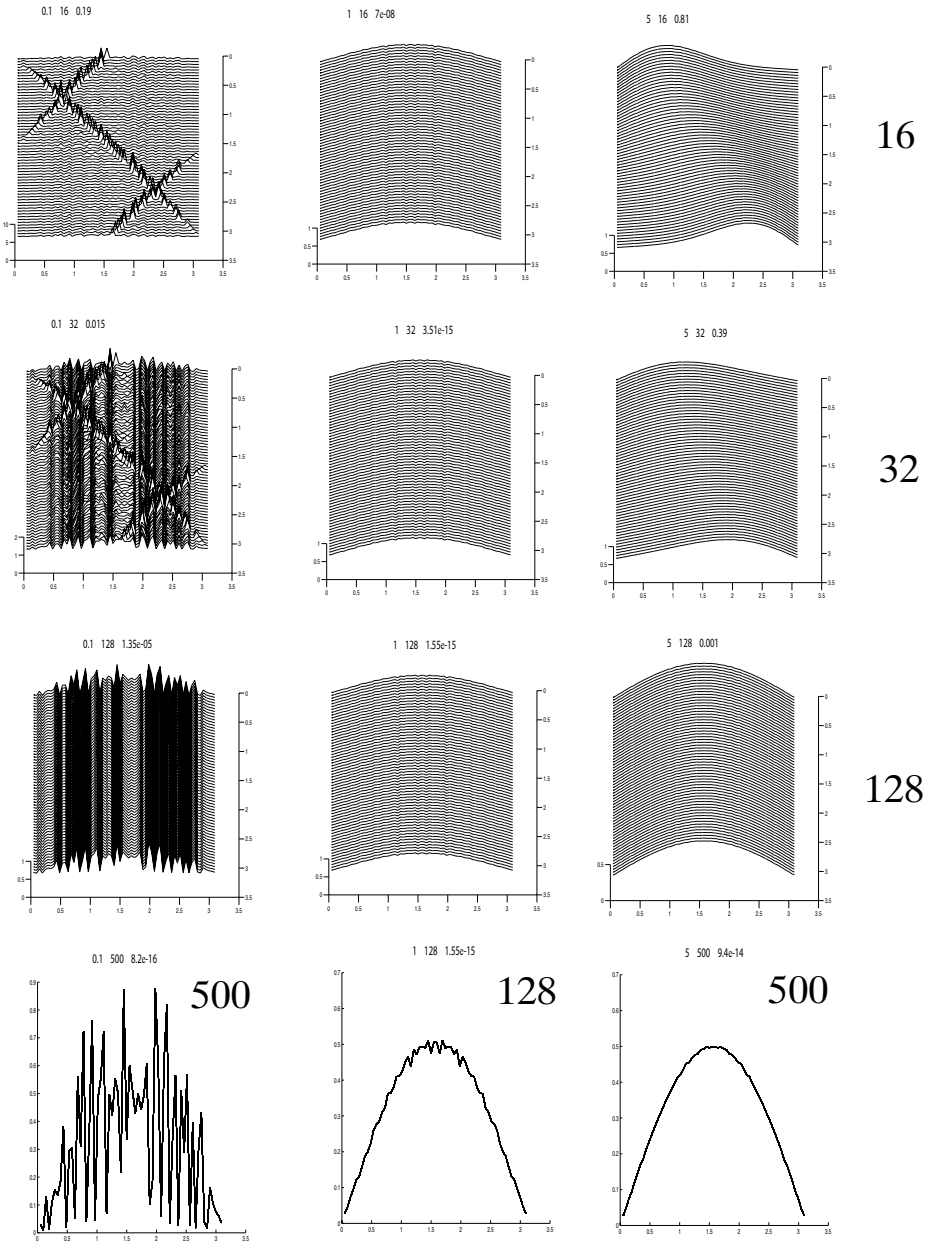

Figure 19. Continuation of Figure 18. The last row gives the views in profile of the graphs for large values of n. The horizontal axis represents θ_{out} and the vertical axis represents the probability density.

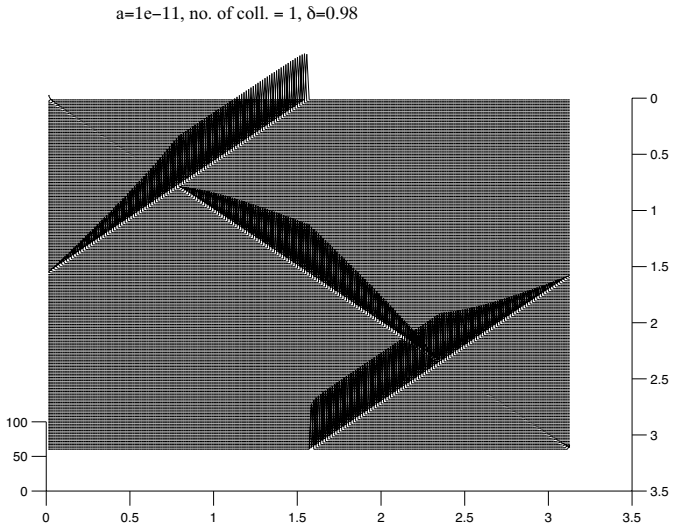

Figure 7. Scattering kernel for the zig-zag microgeometry.

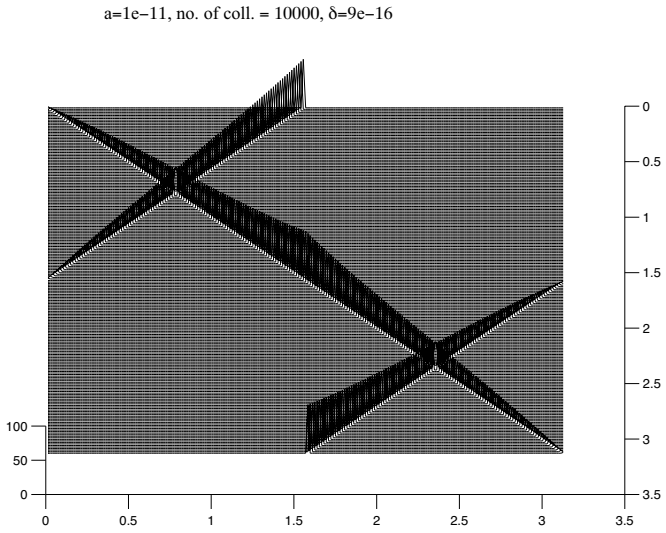

Figure 21. Graph of P_{10000} for the zig-zag microgeometry.

8 Conclusions and Further Questions

We have introduced a probabilistic model of gas-surface interaction, the *random billiard* system, which is obtained through a certain limit procedure from a billiard dynamical system. The model involves a choice of *microgeometry*, which is an ordinary

(i.e., not fractal) geometric relief at a microscale. The signature of a gas-surface interaction model is its *scattering kernel*, denoted $R(\mathbf{v}_{\text{in}} \to \mathbf{v}_{\text{out}})$. The main conclusions are:

- **Basic properties of the random billiard scattering kernel.** We show that the scattering kernel of a general random billiard model satisfies the *reciprocity property*. This can be interpreted as saying that Knudsen's cosine law is a stationary probability distribution of a Markov chain whose transition probabilities are specified by R.
- **Non-uniqueness of the stationary distribution.** Although the cosine law is always stationary, it is not always the only stationary distribution, as we show by means of an example. This example has the property that a numerically stable stationary distribution for R is different from Knudsen's.
- **Approach to stationarity.** On the basis of our numerical experiments, some of which are mentioned in this paper, the non-uniqueness referred to above seems to be rather exceptional. We give a conceptual explanation for this fact, although a precise theoretical characterization of which microgeometries lead to uniqueness will have to await further work. It can be shown analytically that once the stationary distribution of R is unique, then it must be stable. Although this is indeed what we observe numerically by iterating the Markov process defined by R, we also observe that the rate (measured by the number of iterations of R) at which an initial distribution of scattered velocities converges to the cosine law varies greatly with the microgeometry.

When the idealized gas channel consists of a pair of parallel lines on the plane, the Markov process provides in a simple and direct way the probabilistic description of the random motion of individual molecules through the channel. For other channel geometries the relationship between the Markov process and the molecular random flight is more complicated and requires further study.

As noted above, we have both theoretical and numerical evidence to support the believe that the non-uniqueness of stationary post-collision probability distributions is a very exceptional, possibly not physically meaningful situation. If this is correct, a simple but noteworthy conclusion is that the stationary distribution of scattered velocities will not depend in general on the microdetails of the gas-surface interaction. Thus information about these microdetails that are encoded in such transport characteristics as the diffusivity constant has to be sought out in a study of the precise way in which that distribution is achieved.

In other words, we have shown (for the random billiard model) that, as an individual molecule undergoes a random flight inside the channel and its direction at a time t becomes increasingly independent of the direction at a past time t_0, a probability distribution is approached that does not contain information about those microdetails. However, we also show numerically that changes in the microdetails of the random billiard model do have a pronounced influence on the rate at which the limit distribution is achieved. That rate can thus provide a link between the observed diffusivity and the surface microgeometry through the classical expression $\mathcal{D} = \lim_{t\to\infty} \langle \Delta t^2 \rangle / 2t$, used in the form

$$\mathcal{D} = \lim_{N\to\infty} \frac{\left\langle \left(\sum_{n=1}^{N} v_n \tau_n \right)^2 \right\rangle}{2 \left\langle \sum_{n=1}^{N} \tau_n \right\rangle},$$

where v_n is the component of the gas molecule velocity along the length of the channel, τ_n is the time between the n-th and $n+1$-st collisions, and N counts the number of collisions. Notice that the statistics of τ_n and v_n can be obtained from the scattering kernel R and the (macro-) geometry of the channel.

In summary, the physico-chemical meaning of our main results is as follows:

- The Knudsen cosine law for a *single collision* between molecule and channel wall holds at best approximately. The approximation is better the more "dispersing" the microgeometry.
- For *multiple collisions* the cosine law is approached asymptotically as the number of collisions grow, for most microgeometries. The approach is faster the more dispersing the microgeometry.
- The random billiard model always has Knudsen's cosine law as a stationary distribution of post-collision scattered directions. Mathematically, the cosine law is not always its only stationary distribution but microgeometries that admit other stationary distributions besides the cosine law probably are not physically meaningful.
- The random billiard model is the limit, in an appropriate sense, of deterministic systems as the ratio of macro to micro scales goes to infinity.

There are many questions suggested by our approach which are only partially touched on here. From the physico-chemical viewpoint the main problem can be broadly described as trying to understand the connection between the scattering operator $\mathcal{R}$ and the microgeometry of the channel's inner surface, as well as the range of values of parameters under experimental control over which information about those microdetails can be measured. A future study will be devoted to an analysis of a TAP experiment [YOM] in which both diffusion and chemical reaction occur.

We wish to thank John Gleaves and Sergiy Shekhtman for many helpful discussions. We also thank Sergiy Shekhtman for suggesting a great number of improvements and corrections to the text.

References

[ArChMa] G. Arya, H-C. Chang, and E. J. Marginn. *Knudsen Diffusivity of a Hard Sphere in a Rough Slit Pore*, Phys. Rev. Lett., **91**, 026102(4), 2003.

[Ba] H. Babovsky. *On Knudsen flows within thin tubes*, J. Stat. Phys., **44**, Nos. 5/6, 865-878, 1986.

[BGT] C. Börgers, C. Greengard, and E. Thomann. *The diffusion limit of free molecular flow in thin plane channels*, SIAM J. Appl. Math. **52**, No. 4, 1057-1075, 1992.

[Ce] C. Cercignani. The Boltzmann Equation and its Applications, Springer, New York, 1988.

[CeSa] C. Cercignani, D. H. Sattinger. Scaling Limits and Models in Physical Processes, Birkhäuser, 1998.

[CFS] I. P. Cornfeld, S. V. Fomin and Ya. G. Sinai. Ergodic Theory, Springer, 1982.

[Co] M.-O. Coppens. 1999, *Catalysis Today* **53**, 225-243.

[GEK] J.T. Gleaves, J.R. Ebner, T.C. Kuechler. *Temporal analysis of products (TAP)–a unique catalyst evaluation system with submillisecond time resolution*, Catal. Rev. Sci. Engng., (30), 49-116, 1988.

[GYPS] J.T. Gleaves, G.S. Yablonsky, Ph. Phanawadee, Y. Schuurman. *TAP-2: an interrogative kinetics approach*, Appl. Catal., A: General, (160), 55-87, 1997.

[HK] B. Hasselblatt and A. Katok. Introduction to the Modern Theory of Dynamical Systems, Encyclopedia of Mathematics and its Applications, 54, Cambridge University Press, 1995.

[Ke] F. Keil. *Diffusion und Chemische Reaktionen in der Gas/Feststoff*, Katalyse, Springer, 1999.

[KR] J. Kärger and D. M. Ruthven. *Diffusion in zeolites and other microporous solids*, Wiley, New York, 1992.

[KS] A. Katok and J-M. Strelcyn. Invariant Manifolds, Entropy and Billiards; Smooth Maps with Singularities, Lecture Notes in Mathematics, 1222, Springer 1986.

[Kn] M. Knudsen. Kinetic Theory of Gases – Some Modern Aspects, Methuen's Monographs on Physical Subjects, London, 1952.

[MaCo] K. Malek and M.-O. Coppens. 2001, *Phys. Rev. Lett.* **87**, 125505.

[Re] D. Revuz. Markov Chains, North-Holland/Elsevier, 1975.

[Ru1] D. Ruelle. *Positivity of entropy production in the presence of a random thermostat*, J. Statist. Phys. **85** 1-23 (1996).

[Ru2] D. Ruelle. *Smooth Dynamics and New Theoretical Ideas in Nonequilibrium Statistical Mechanics*, J. Statist. Phys. **95** 393-468 (1999).

[SSH] S. B. Santra, B. Sapoval, O. Haeberlé. *Lévy distribution of collisions for Knudsen diffusion in fractal pores.*

[SNQ] V.P. Sokhan, D. Nicholson, and N. Quirke. J. Chem. Phys., 117, 8531 (2002).

[St] E. M. Stein. Harmonic Analysis, Princeton Mathematical Series, 43, 1993, Princeton University Press.

[Ta] S. Tabachnikov. Billiards, Panoramas et Synthèses, No. 1, Société Mathématique de France, 1995.

[Wa] P. Walters. An Introduction to Ergodic Theory, Springer, 1982.

[YOM] G.S. Yablonsky, M. Olea, G.B. Marin. *Temporal analysis of products: basic principles, applications, and theory*, Journal of Catalysis 1-2, 120-134, May-June 2003.